The Stability of Direct Carbon Fuel Cells with Molten Sb and Sb–Bi Alloy Anodes

Abhimanyu Jayakumar
Dept. of Chemical and Biomolecular Engineering, University of Pennsylvania, Philadelphia, PA 19104

Ashay Javadekar
Dept. of Chemical Engineering, University of Delaware, Newark, DE 19716

Jacob Gissinger and John M. Vohs
Dept. of Chemical and Biomolecular Engineering, University of Pennsylvania, Philadelphia, PA 19104

George W. Huber
Dept. of Chemical Engineering, University of Massachusetts, Amherst, MA 01003

Raymond J. Gorte
Dept. of Chemical and Biomolecular Engineering, University of Pennsylvania, Philadelphia, PA 19104

DOI 10.1002/aic.13965
Published online November 26, 2012 in Wiley Online Library (wileyonlinelibrary.com).

The long-term stability of direct carbon fuel cells, based on solid oxide fuel cells with molten Sb and Sb–Bi anodes, was examined for operation with activated charcoal, rice starch, and bio-oil fuels at 973 K. With intermittent stirring of the fuel–metal anode interface, the anode performance was stable, and reasonable power densities (~250 mW/cm^2) were achieved for periods up to 250 h. With Sc-stabilized zirconia, severe thinning of the electrolyte occurred in regions of high current flow. No electrolyte thinning was observed with yttria-stabilized zirconia as the electrolyte operating at the same current densities. © 2012 American Institute of Chemical Engineers *AIChE J,* 59: 3342–3348, 2013
Keywords: fuel cells, coal, energy, electrochemistry, catalysis, molten antimony, bio-oil

Introduction

Solid oxide fuel cells (SOFCs) are based on ceramic electrolytes that are oxygen-ion conductors. Therefore, in these fuel cells, the electrochemical conversion of any combustible fuel, including carbonaceous solids such as coal and biomass, is at least theoretically possible. The generation of electrical power by direct utilization of solid fuels in an SOFC would also provide significant benefits, if it could be practiced on a large scale. The efficiency of an SOFC can be very high, with negligible NO_x emissions. Moreover, if CO_2 sequestration is required, the exhaust gas from the anode is highly concentrated, allowing for easy CO_2 capture.[1,2] Finally, direct utilization of solid fuels would greatly simplify the overall conversion process by eliminating the need for gasification and steam reforming steps.[3]

In any SOFC, O_2 from the air is reduced at the cathode to produce O^{2-} anions, according to Eq. 1.

$$O_2 + 4e^- \rightarrow 2O^{2-} \tag{1}$$

As shown by this equation, the cathode must catalyze the dissociation of O_2 and must be an electronic conductor to supply electrons for the reaction. The O^{2-} anions then pass through the dense ceramic electrolyte, which must be an electronic insulator to generate current through movement of the O^{2-} anions only. Finally, the O^{2-} anions oxidize the fuel at the anode; if that fuel is carbon, the anode reaction is given by Eq. 2.

$$C + 2O^{2-} \rightarrow CO_2 + 4e^- \tag{2}$$

The overall fuel-cell reaction is $C + O_2 \rightarrow CO_2$, but the electrons produced at the anode have a higher potential energy from those consumed at the cathode.

The performance of SOFC operating on carbon is almost always limited by the transfer of oxide ions from the electrolyte to the solid fuel.[4] Various approaches have been taken to facilitate this transfer,[5–8] one of the most promising involving the use of molten-metal electrodes.[9–11] In this case, the anode reaction can be split into the following two reactions, given by Eqs. 3 and 4.

$$nM + xO^{2-} \rightarrow M_nO_x + 2xe^- \tag{3}$$

$$(x/2)C + M_nO_x \rightarrow (x/2)CO_2 + nM \tag{4}$$

The first step (Eq. 3) is the oxidation of a portion of the metal in the anode, which occurs at the electrolyte–anode interface. The oxidized metal is then transported (via natural

Correspondence concerning this article should be addressed to R. J. Gorte at gorte@seas.upenn.edu.

convection or mechanical mixing) to the fuel where the carbon is oxidized, and the metal oxide is reduced (Eq. 4). Only the first step in this sequence is electrochemical. The majority of studies in this area have utilized Sn as the metal.[9,10] Unfortunately, there is evidence that a solid SnO_2 layer forms at the electrolyte interface during fuel-cell operation, inhibiting further transfer of the oxygen from the electrolyte, resulting in high electrode losses.[12] While this can be avoided using a molten metal, such as Ag, with some oxygen solubility and no stable bulk oxide phase at SOFC operating temperatures, electrode impedances can still be high due to slow diffusion of oxide ions within the molten metal.[13]

The metal that provided the most intriguing results as an anode for this type of direct carbon fuel cell (DCFC) was Sb.[14] Both Sb (melting point 903 K) and Sb_2O_3 (melting point 929 K) have melting points below the temperatures typically used for SOFC operation, 973–1073 K, which precludes the formation of a solid oxide film at the electrolyte–anode interface as in the case of Sn. Based on previous experiments in our laboratory, the impedance of molten Sb electrodes are very low, less than 0.1 Ω cm^2 at 973 K,[11] and reasonably independent of the $Sb:Sb_2O_3$ ratio.[15] Although the Nernst potential for Sb oxidation is lower compared to that for C oxidation, 0.75 V vs. $\sim$1 V at 973 K, this difference in oxidation potentials makes the reduction of Sb_2O_3 by the solid carbonaceous fuels thermodynamically spontaneous. Indeed, carbon is a well-known reductant for the production of metallic Sb from Sb_2O_3 as demonstrated by the fact that charcoal was used for this purpose on an industrial scale more than 100 years ago.[16]

In a previous study of an SOFC with a molten Sb anode, stable generation of electrical power was demonstrated for a period of approximately 13 h using ash-free sugar char as the fuel.[11] Unfortunately, longer tests were not possible in this study, because the experimental configuration did not allow additional solid fuel to be added after the initial charge of sugar char had been consumed. Also, because the solid fuels were placed directly on top of the Sb within the anode compartment, without any stirring, fuels that formed an ash layer were prevented from reducing Sb_2O_3 after only a fraction of the fuel had been oxidized. This was due to poor contacting between the fuel and the Sb_2O_3 that formed by oxidation of the Sb at the electrolyte interface.

In this article, we describe the results of a study of the long-term stability (>200 h) of SOFCs with anodes based on molten Sb and on Sb–Bi alloys, operating on a variety of carbonaceous fuels, including activated charcoal, a bio-oil, and rice starch. This was accomplished by modifying the experimental setup to allow the periodic addition of fuel with intermittent stirring of the molten anode to break up any barrier due to ash formation. We observe relatively small variations in performance with time that may be due to incomplete mixing in the compartment. Cells with both yttria-stabilized zirconia (YSZ) and scandia-stabilized zirconia (ScSZ) electrolytes were evaluated. ScSZ electrolytes were found to undergo thinning in regions where the electrochemical reaction occurs. Fortunately, no such thinning was observed with YSZ, so that long-term operation of such DCFCs with Sb-based anodes should be possible.

Experimental

The molten metal anodes in the fuel cells used here consisted simply of having the molten metal in contact with the bare electrolyte surface. Therefore, the ceramic component of the cells consisted of just the electrolyte with the cathode on one side. The cathode-electrolyte bilayer wafers were constructed using tape-casting methods that have been described in other articles.[17,18] Briefly, tapes, with and without pore formers, were laminated and fired to produce a bilayer wafer of the electrolyte material with one layer porous and the other dense. The circular porous layer was 0.67 cm in diameter, whereas the dense electrolyte layer was 1.4 cm in diameter. The electronically conductive cathode was prepared from the porous layer by infiltration of nitrate salts to produce a composite that was 35 wt % $La_{0.8}Sr_{0.2}FeO_3$ (LSF). X-ray diffraction was used to confirm that the LSF had the proper perovskite structure following calcination to 1123 K.[19,20]

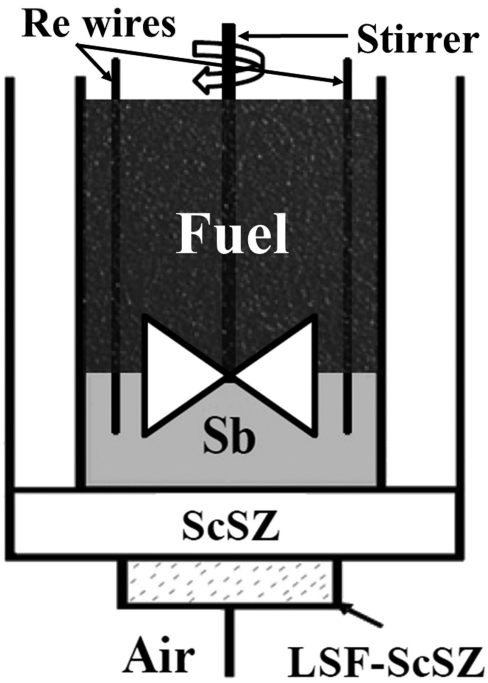

Figure 1. Schematic of the experimental setup of a DCFC with a molten Sb anode.

The two electrolyte materials tested in this study were 10% ScSZ and 8% YSZ. Although ScSZ is significantly more expensive than YSZ, it is mechanically stronger and has a higher ionic conductivity.[21] The cells made with ScSZ had 100-μm-thick electrolytes, whereas the YSZ cells had electrolytes that were 160-μm thick, made by laminating two 80-μm tapes. In both ScSZ and YSZ cells, the porous cathode was 50-μm thick.

The experimental apparatus is shown schematically in Figure 1 and was similar to that used in an earlier study of electrochemical energy storage, where mixing of the molten Sb/Sb_2O_3 mixture was critical.[15] The fuel cell was attached to the end of an alumina tube with the cathode side exposed, using a ceramic adhesive (Aremco Ceramabond 552). Silver paste and wires were used to make electrical connections to the cathode. Next, metal powder was added into the alumina tube, making contact with the anode side of the electrolyte surface by gravity. Experiments with pure Sb used 10 g of Sb powder (-100 mesh, 99.5%, Alfa Aesar), whereas experiments with the Sb–Bi alloy used a mixture of 8 g of Sb and 3.45 g of Bi (-100 mesh, 99%, Sigma–Aldrich) to produce

Table 1. Concentration of Products in Pyrolysis Oil (wt %)

Gas chromatograph (GC) detected compounds	
Hydroxyacetaldehyde	1.46
Acetic acid	9.02
Hydroxyacetone	1.25
1-Hydroxy-2-butanone	0.34
1,2-Butanediol	0.30
Gamma gutyrolactone	0.55
Phenol	0.12
3-Methyl-1,2-cyclopentanedione	0.68
Guaiacol	0.56
High performance liquid chromatography (HPLC) detected compounds	
C6 sugars	0.20
Levoglucosan	3.98
Formic acid	1.52
Hydroxymethyl fufural	0.93
Furfural	0.28
GC and HPLC identifiable carbon compounds	21.19
Water content	30.27
Pyrolytic lignin	39.49
Total identified products	90.95

an alloy that was 20 mol % Bi. Rhenium wires were inserted into the anode for current collection. The Sb–Sb_2O_3 anode is highly conductive, so current collection was not a problem, and the positioning of the Re wires in the anode did not affect the results. After inserting an alumina stirring rod to the anode–fuel interface, the top end of the alumina tube was plugged with glass wool. Finally, the fuel cell was placed in a tube furnace and heated to 973 K.

The powdered carbonaceous fuels were added directly onto the anode. Biomass fuels were added as a 40% by weight mixture with charcoal (Supelco). Fuel cell tests were conducted using an initial charge of 1.5 g of fuel, with further 0.5-g fuel additions made every 6–10 h of cell operation. Stirring of the anode–fuel interface was carried out for 2–5 min before and after every fuel addition. To obtain a better measure of the amount of fuel that was added to the anode compartment, each of the fuels was briefly heated to 873 K in an inert gas to drive off volatile gases prior to measuring the fuel weight added to the cell. In a typical 200-h experiment, the total amount of fuel added to the anode was ~13 g, of which ~5 g was recovered at the end of the experiment. As a point of reference, 4.0 g of pure C would be required to produce a current of 500 mA/cm^2 for 200 h, with the current density referenced to the active area of our cathodes, 0.353 cm^2. The difference between the amounts of fuel that were consumed (~8 g) and the electron balance (4 g) is partially associated with oxygen in the fuel and partially to remaining volatility in the fuel.[22] Also, excess fuel was always maintained in the cell to compensate for unpredictable losses and to provide a barrier for Sb and mainly, Sb_2O_3 vaporization.

The biomass fuels used were rice starch (Sigma–Aldrich) and a bio-oil. This pyrolysis oil was obtained from sugar maple in an auger/transport bed reactor designed by Renewable Oil International LLC (ROI). The reactor system is built around an adiabatic reactor zone that had three inlets: (1) a solid heat carrier, (2) dried and ground biomass, and (3) a N_2 sweep gas. A stainless steel shot with a size of about 2 mm served as the heat carrier. During production, the heat carrier and char were carried away from the reactor zone to the char separation system using another auger. Pyrolysis vapors from the reactor zone were then sent to a vapor recovery system that consisted of a tar trap, eight condensers and an electrostatic precipitator in series. The pyrolysis oils were then filtered with a 1.4-μm filter to remove char impurities,[23] and the yield of bio-oil produced in this reactor was 53 wt %. A range of techniques were used to characterize the bio-oil as shown in Table 1. The detected bio-oil composition included 39.5 wt % pyrolytic lignin, 30.3 wt % water, 9.4 wt % acetic acid, and 11.8 wt % other measured oxygenated organic molecules.

V–i polarization curves and impedance measurements in this study were performed using a Gamry Instruments Potentiostat. As reference electrodes are unreliable,[24] all potentials reported in this article were between the cathode and anode. Unless otherwise stated, the current densities reported in this article were normalized to the external area of the cathode. The *V–i* polarization curves were obtained by ramping through the applied voltages from the open-circuit voltage (OCV) of 0.75–0 V (short circuit) at a ramp rate of 10 mV/s and measuring the corresponding currents. Impedance spectra were performed galvanostatically in the frequency range from 300 kHz to 0.1 Hz with an a.c. perturbation of 1 mA. Scanning electron microscopy (SEM) was performed using a JEOL 7500F HRSEM.

Results

Cells with ScSZ electrolytes

In the previous work, it was shown that relatively high power densities are possible using a molten Sb anode in an SOFC and that carbonaceous fuels preloaded into the anode compartment can be used to generate electricity.[11] However, the testing rig used in that study did not have the capability of adding fuel during the course of the measurements and, therefore, could not be used for long-term testing. Figure 2 shows results from a 200-h experiment in which the current density, normalized to the external area of the cathode, was monitored while holding the cell potential at 0.5 V, with intermittent addition of various fuels. The arrows indicate the times at which 0.5 g increments of fuel (60 wt % charcoal and 40 wt % of either rice starch or bio-oil) were

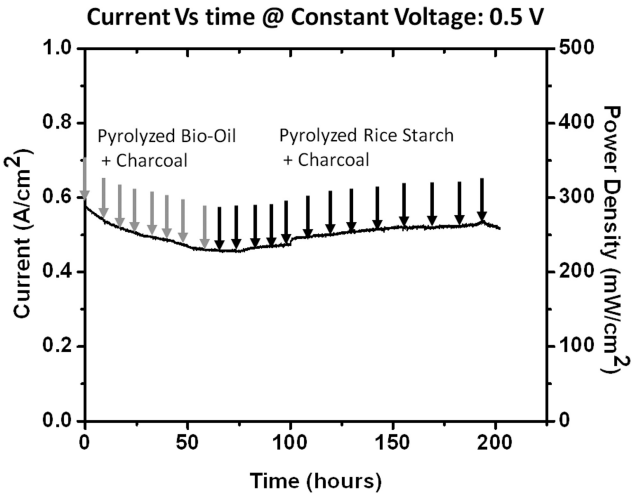

Figure 2. Long-term performance plot for the DCFC with a pure Sb anode and a ScSZ electrolyte.

The DCFC is run on three different solid fuels, pyrolyzed bio-oil, pyrolyzed rice starch, and activated charcoal. Current is being generated at a constant voltage of 0.5 V.

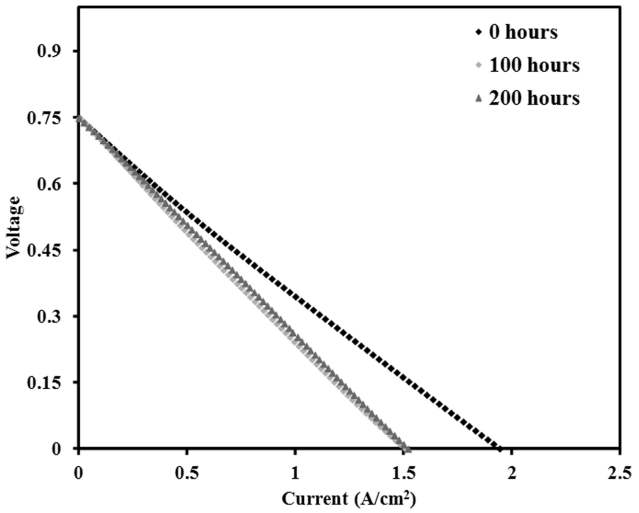

Figure 3. *V–i* polarization curves for the DCFC with a pure Sb anode and a ScSZ electrolyte.

added. The normalized power densities are reported on the right side. The cell used in this experiment had a 100-μm ScSZ electrolyte, with an LSF–ScSZ composite cathode and 10 g of Sb as the anode. The current and power densities initially drifted downward during the first 70 h, from a current density of 580 mA/cm^2 and power density of 290 mW/cm^2, to a current density of 460 mA/cm^2 and power density of 230 mW/cm^2, after which the performance started to increase.

To gain insight into the reasons behind the drifting current densities in Figure 2, *V–i* polarization curves and impedance spectra were collected at 0, 100, and 200 h, with the data shown in Figures 3 and 4. As shown in Figure 3, the OCV was 0.75 V at all times, in agreement with the expected Nernst potential for Sb oxidation to Sb_2O_3 at 973 K. The *V–i* relationships were nearly linear and the slope of the *V–i* relationship, which is the total area specific resistance of the cell, increased from an average initial value of 0.38 to 0.50 Ω cm^2 after 100 h. The *V–i* relationships at 100 and 200 h were virtually unchanged.

The corresponding open-circuit impedance data at these three times are shown in Figure 4. At 0 h, the Nyquist plot of the impedance spectrum has a zero-frequency intercept with the abscissa at 0.38 Ω cm^2, identical to the slope of the *V–i* plot, as expected. The ohmic resistance of the cell, given by the high-frequency intercept with the abscissa, is 0.22 Ω cm^2, a value equal to the calculated resistance of a 100-μm ScSZ electrolyte.[21] The difference between these resistances, 0.16 Ω cm^2, corresponds to the losses associated with the two electrodes. Separate measurements of identical LSF–ScSZ cathodes indicate that the resistance of this electrode should be 0.06 Ω cm^2 at 973 K[21] and will remain more or less unchanged over the time-scale of the test,[20] implying that the anode losses are on the order of 0.1 Ω cm^2. After 100 and 200 h, the impedance spectra show that the total electrode losses increased from 0.16 to $\sim$0.25 Ω cm^2. This increase is almost certainly associated with the molten Sb–Sb_2O_3 anode, possibly due to a buildup of oxide at the electrolyte interface. Although, in a previous study, it was shown that the impedance of a molten Sb electrode does not change significantly with the Sb:Sb_2O_3 ratio over a fairly wide range of compositions,[15] that study was carried out with continuous vigorous stirring of the molten electrode. In this study, except for the intermittent mechanical mixing when fuel was added, natural convection was relied on for mixing the oxide into the metal anode, and it is likely that there was a buildup of the oxide at the electrolyte interface.

Of greater concern in Figure 4 is the decreasing ohmic resistance that declined to 0.17 Ω cm^2 after 100 h and to 0.13 Ω cm^2 after 200 h. As the ohmic losses are associated with the electrolyte and must be at least as high as the resistance of the electrolyte, a decrease in this value suggests that the electrolyte has become significantly thinner during the measurements. This was later confirmed by SEM, which showed that the dense ScSZ electrolyte had gone from an initial thickness of 100 to 73 μm over the 200-h experiment. As will be discussed later in this article, this thinning of the electrolyte only occurred in the region between the cathode and the molten anode, implying that it is due to an electrochemical process and not simply corrosion of ScSZ in the molten Sb–Sb_2O_3 mixture. To further ensure that the thinning of the electrolyte is purely electrochemical in nature, a ScSZ electrolyte was exposed to Sb–Sb_2O_3 mixtures at 973 K for more than 600 h in another experiment. After this experiment in which no current was drawn, the ScSZ electrolyte sample on SEM analysis revealed no change in the thickness of the electrolyte. This means that the thinning of the electrolyte occurs only when current is drawn and not by corrosion or dissolution of the electrolyte into the anode melt.

In a previous study of mixed-metal anodes,[25] the electrode performance characteristics followed that of the most easily oxidized metal. In the case of Sb–Bi mixtures, the OCV was close to that for the oxidation of Sb, $\sim$0.738 V; when the Bi–Sb cell was operated in a "battery" mode, the Bi remained metallic and in contact with the electrolyte until all of the Sb was oxidized and floated to the top. The Bi–Sb system is of interest for this study in that the buildup of oxide near the electrolyte interface might be avoided with a denser mixed-metal electrode. Long-term results for a cell with an anode containing a 20–80 mol % mixture of Bi and Sb are shown in Figure 5. While the initial current and power densities at 0.5 V were somewhat lower in this cell, in part due to the slightly lower OCV of the alloy, the

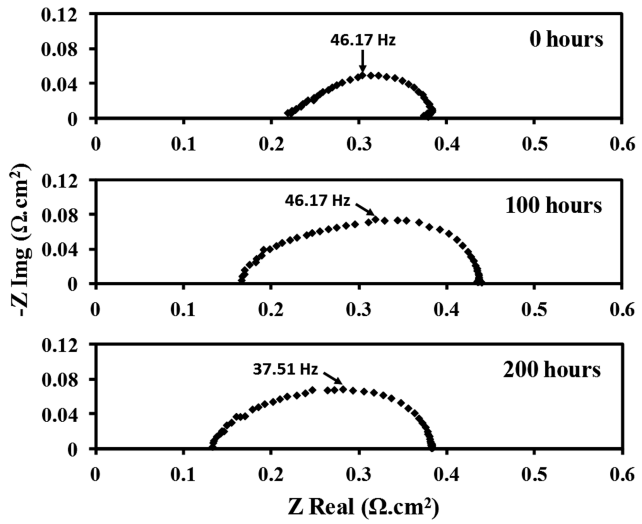

Figure 4. Nyquist impedance spectra for the DCFC with a pure Sb anode and a ScSZ electrolyte.

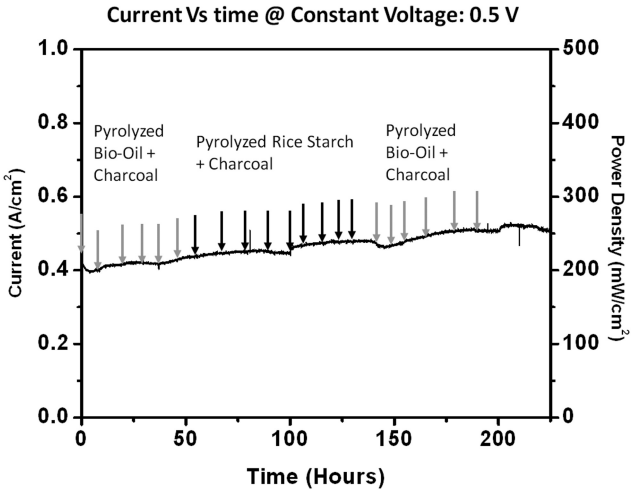

Figure 5. Long-term performance plot for the DCFC with a Sb–Bi alloy anode and a ScSZ electrolyte.

The DCFC is run on three different solid fuels, pyrolyzed bio-oil, pyrolyzed rice starch, and activated charcoal. Current is being generated at a constant voltage of 0.5 V.

performance was more stable, showing only a gradual increase in current density with time, from 400 mA/cm^2 to greater than 500 mA/cm^2 after 225 h. This observation lends support to the hypothesis that the initial downward drift of the current density in Figure 2 is due to a buildup of oxide at the electrolyte interface.

As in the case for the cell with the pure Sb anode, the primary reason for the increasing current densities over time was a decreasing ohmic resistance. Indeed, the loss of ScSZ electrolyte was even more severe with the Bi–Sb mixture than it was with the pure Sb electrode. Figure 6 shows an SEM image of a cross-section of the electrolyte, near the cathode boundary. Because some Ag paste spilled over from the cathode onto the dense electrolyte, lines have been drawn on the image to help the reader see the locations of the various boundaries. The image in Figure 6 shows that the ScSZ electrolyte away from the cathode remains 100-μm thick, indicating that the ScSZ is not etched by the molten metal in the absence of current. However, beneath the cathode, the electrolyte had thinned dramatically, to a value of only 24 μm. It is interesting to notice that the shape of the molten-metal/ScSZ interface is similar to the expected field lines at an electrode–electrolyte interface with asymmetric placement of electrodes.[26,27] Therefore, the thinning process must be electrochemical in nature and related to the amount of charge passed through the electrolyte.

Cells with YSZ electrolytes

The severe loss of electrolyte material found with the ScSZ would prevent any practical application of this technology. To determine whether damage to the electrolyte depends on the particular electrolyte that is used, we performed a long-term test on a cell with a YSZ electrolyte and 10 g of Sb as the anode. Again, the test was performed with intermittent addition of fuel, briefly stirring before and after addition of the solids. Because the ionic conductivity of YSZ is lower than that of ScSZ and the YSZ cells had a thicker electrolyte, the cell performance was modest compared to that for the ScSZ cells. To mimic the conditions experienced by the ScSZ electrolyte, the long-term experiment with YSZ was carried out at a constant current density of 500 mA/cm^2, rather than at constant cell potential. Furthermore, because the aim of this experiment was to pass a similar amount of charge through the YSZ electrolyte, only a single Re wire was used for anode current collection, adding an additional ohmic contribution to the V–i relationship in the cell. With these conditions, the cell potential over the course of 270 h of operation was 0 V, fluctuating between $\pm$0.05 V.

An SEM image of the YSZ electrolyte cross-section after the 270-h test, near the cathode boundary, is shown in Figure 7. Unlike the case with the ScSZ electrolyte, there is no evidence for thinning of the YSZ electrolyte and its appearance between the cathode and the molten metal is identical to that of the YSZ that is away from the cathode. These data demonstrate that electrolyte etching with ScSZ is related to the Sc in some manner and does not appear to occur with Y doping.

Discussion

The results obtained in this study demonstrate that the direct utilization of biomass and other solid fuels in an SOFC is possible using a molten-Sb electrode. As discussed in more detail elsewhere,[15] the theoretical electrical

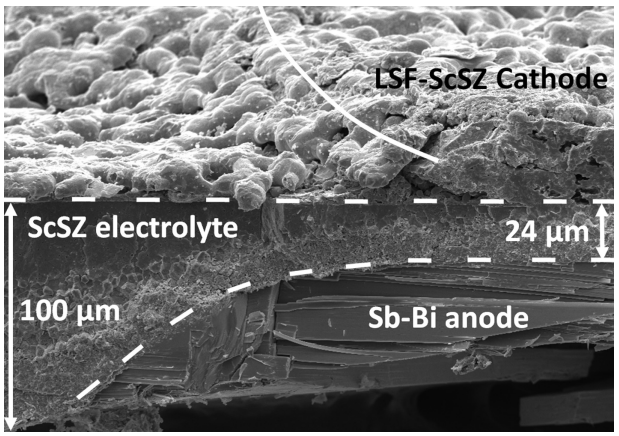

Figure 6. SEM image of the cell cross-section after the long-term test of the DCFC with a Sb–Bi alloy anode and a ScSZ electrolyte.

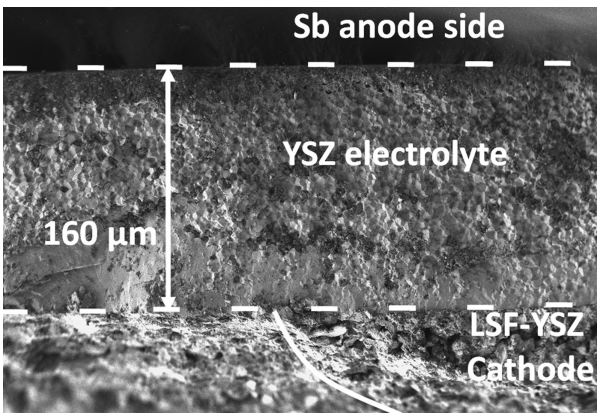

Figure 7. SEM image of the cell cross-section after the long-term test of the DCFC with a pure Sb anode and a YSZ electrolyte.

efficiency of a cell based on Sb, equal to $\Delta G/\Delta H$, is only 0.65; however, the remaining energy associated with fuel oxidation could be captured as heat and utilized in other ways. Because Sb_2O_3 is effective in assisting the conversion of the fuels, oxidizing even graphite at temperatures below 1073 K,[11] NO_x emissions will be minimal. Impurities carried in with the fuel are a concern; however, with the exception of metals that could form alloys with Sb, most oxides can be separated by gravity. Sb does form a sulfide, but Sb_2S_3 has a melting point of 823 K and can be easily converted back to the metal. Obviously, stack design with molten Sb will be a challenge, but the actual cells could be simpler in that there is effectively no separate anode layer to design.

As the impedance of the molten-Sb electrode is low, $\sim$0.1 Ω cm^2 at 973 K, cell performance will be determined by the cathode and electrolyte losses. While the degradation of the ScSZ electrolyte suggests that the choice of electrolyte material will be dictated by stability, electrolyte losses can still be minimized through the use of thin YSZ electrolytes. Indeed, in conventional SOFC, 10-μm electrolytes are common and would add negligible resistance to cells operating at 973 K or higher temperatures.

The large difference in the stabilities of ScSZ and YSZ against electrochemical etching by the molten Sb is noteworthy. Sc^{3+} cations are much smaller than Y^{3+} cations and are known to have a high mobility in the lattice of cubic ZrO_2.[28] Therefore, we hypothesize that this mobility leads to the migration of Sc^{3+} cations out of the electrolyte and into the molten metal. A similar net migration of Sc^{3+} out of the electrolyte has been reported for ScSZ in contact with B_2O_3.[29] Loss of Sc from the ZrO_2 lattice could in turn destabilize the cubic structure, causing mechanical stresses that could cause flaking of the zirconia from the surface of the electrolyte. The reason behind etching being so much larger with Bi–Sb mixtures is unknown, but it may simply be the result of minimizing the amount of oxide that is in the vicinity of the active electrolyte interface.

It is interesting to compare the etching phenomenon of this study with recent reports of large morphological changes in YSZ that occur at higher temperatures and current densities.[30] That work attributed the effect to a supersaturation of oxygen vacancies within the electrolyte. Whether these phenomena are related is unknown at this time.

Clearly, more work needs to be done to demonstrate the practicality of direct-carbon fuel cells based on molten-Sb anodes. However, the results of this study further demonstrate the potential of this technology for achieving breakthrough efficiencies and improved environmental impact with complex fuels, making this a promising area for future development.

Conclusion

The generation of electricity through the direct oxidation of various solid fuels, including rice starch, charcoal, and bio-oil, has been demonstrated using an SOFC with a molten-Sb anode. These cells are able to generate high power densities with stable anode performance. Although YSZ electrolytes exhibit good stability, an electrochemical etching phenomenon was observed with ScSZ that would prevent the use of ScSZ in this application.

Acknowledgments

This work was supported as part of the Catalysis Center for Energy Innovation, an Energy Frontier Research Center funded by the U.S. Department of Energy, Office of Science, Office of Basic Energy Sciences under Award no. DE-SC0001004.

Literature Cited

1. Cao DX, Sun Y, Wang GL. Direct carbon fuel cell: fundamentals and recent developments. *J Power Sources*. 2007;167:250–257.
2. Program on Technology Innovation: Systems Assessment of Direct Carbon Fuel Cells Technology, Electric Power Research Report Number 1016170, EPRI, Alto, CA, 2008.
3. Li S, Lee AC, Mitchell RE, Gür TM. Direct carbon conversion in a helium fluidized bed fuel cell. *Solid State Ionics*. 2008;172:1549–1552.
4. Nürnberger S, Bußar R, Desclaux P, Franke B, Rzepka M, Stimming U. Direct carbon conversion in a SOFC-system with a non-porous anode. *Energy Environ Sci*. 2010;3:150–153.
5. Lipilin AS, Balachov II, Dubois LH, Sanjurjo A, McKubre MC, Crouch-Baker S, Hornbostel MD, Tanzella FL. Liquid anode electrochemical cell. US Patent 8,01,310, 2012.
6. Nabae Y, Pointon KD, Irvine JTS. Electrochemical oxidation of solid carbon in hybrid dcfc with solid oxide and molten carbonate binary electrolyte. *Energy Environ Sci*. 2008;1;148–155.
7. Jain SL, Lakeman JB, Pointon KD, Marshall R, Irvine JTS. Electrochemical performance of a hybrid direct carbon fuel cell powered by pyrolysed MDF. *Energy Environ Sci*. 2009;2:687–693.
8. Lee AC, Li S, Mitchell RE, Gür TM. Conversion of solid carbonaceous fuels in a fluidized bed fuel cell. *Electrochem Solid-State Lett*. 2008;11(2):B20–B23.
9. Tao T, Bateman L, Bentley J, Slaney M. Liquid tin anode solid oxide fuel cell for direct carbonaceous fuel conversion. *ECS Trans*. 2007;5:463–472.
10. Tao T, Slaney M, Bateman L, Bentley LJ. Anode polarization in liquid tin anode solid oxide fuel cell. *ECS Trans*. 2007;7:1389–1397.
11. Jayakumar A, Küngas R, Roy S, Javadekar A, Vohs JM, Buttrey DJ, Gorte RJ. A direct carbon fuel cell with a molten antimony anode. *Energy Environ Sci*. 2011;4:4133–4137.
12. Jayakumar A, Lee S, Hornes A, Vohs JM, Gorte RJ. A comparison of molten Sn and Bi for solid oxide fuel cell anodes. *J Electrochem Soc*. 2010;157:B365–B369.
13. Javadekar A, Jayakumar A, Pujara R, Vohs JM, Gorte RJ. Molten silver as a direct carbon fuel cell anode. *J Power Sources*. 2012;214:239–243.
14. Jayakumar A, Vohs JM, Gorte RJ. Molten-metal electrodes for solid oxide fuel cells. *Ind Eng Chem Res*. 2010;49(21):10237–10241.
15. Javadekar A, Jayakumar A, Gorte RJ, Vohs JM, Buttrey DJ. Energy storage in electrochemical cells with molten Sb electrodes. *J Electrochem Soc*. 2012;159(4):A386–A389.
16. DeCew JA. Metallurgical and Chemical Engineering, Vol. 16, no. 8. New York: McGraw-Hill Publishing Co Inc., 1917:444–449.
17. Park S, Gorte RJ, Vohs, JM. Tape cast solid oxide fuel cells for the direct oxidation of hydrocarbons. *J Electrochem Soc*. 2001;148:A443–A447.
18. Vohs JM, Gorte RJ. High-performance SOFC cathodes prepared by infiltration. *Adv Mater*. 2009;21:943–956.
19. Huang YY, Vohs JM, Gorte RJ. Fabrication of Sr-doped $LaFeO_3$–YSZ composite cathodes. *J Electrochem Soc*. 2004;151:A646–A651.
20. Wang W, Gross MD, Vohs JM, Gorte RJ. The stability of LSF–YSZ electrodes prepared by infiltration. *J Electrochem Soc*. 2007;154:B439–B445.
21. Küngas R, Vohs JM, Gorte RJ. Effect of the ionic conductivity of the electrolyte in composite SOFC cathodes. *J Electrochem Soc*. 2011;158(6):B743–B748.
22. Wang N, Low MLD. Spectroscopic studies of carbons. *XIX. The charring of sucrose. Mater Chem Phys*. 1990;26(5):465–481.
23. Javaid A, Ryan T, Berg G, Pan X, Vispute T, Bhatia S, Huber GW, Ford DM. Removal of char particles from bio-oils by microfiltration. *J Membr Sci*. 2010;363(1–2):120–127. DOI: 10.1016/j.memsci.2010.07.021.
24. McIntosh S, Vohs JM, Gorte RJ. A study of direct-oxidation SOFC anodes by impedance spectroscopy. *J Electrochem Soc*. 2003;150:A1305–A1312.
25. Javadekar A, Jayakumar A, Gorte RJ, Vohs JM, Buttrey DJ. Characteristics of molten alloys as anodes in solid oxide fuel cells. 2011;158(12):B1472–B1478.
26. Adler SB. Reference electrode placement in thin solid electrolytes. *J Electrochem Soc*. 2002;149(5): E166–E172.

27. Adler SB, Henderson BT, Wilson MA, Taylor DM, Richards RE. Reference electrode placement and seals in electrochemical oxygen generators. *Solid State Ionics*. 2000;134:35–42.
28. Idris MA, Bak T, Li S, Nowotny J. Effect of segregation on surface and near-surface chemistry of yttria-stabilized zirconia. *J Phys Chem C*. 2012;116:10950–10958.
29. Kishimoto H, Sakai N, Yamaji K, Horita T, Xiong YP, Brito ME, Yokokawa H. Destabilization of cubic-stabilized zirconia electrolyte induced by boron oxide under reducing atmosphere. *J Mater Sci*. 2009;44:639–646.
30. Kim SW, Kim SG, Jung JI, Kang SJL, Chen IW. Enhanced grain boundary mobility in yttria-stabilized cubic zirconia under an electric current. *J Am Ceram Soc*. 2011;94(12):4231–4238.

Manuscript received July 3, 2012, and revision received Sept. 28, 2012.